A&A 511, A21 (2010)
DOI: 10.1051/0004-6361/200912700

Astronomy & Astrophysics

The HARPS search for southern extra-solar planets

XIX. Characterization and dynamics of the GJ 876 planetary system⋆,⋆⋆

A. C. M. Correia[1,2], J. Couetdic[2], J. Laskar[2], X. Bonfils[3], M. Mayor[4], J.-L. Bertaux[5], F. Bouchy[6], X. Delfosse[3], T. Forveille[3], C. Lovis[4], F. Pepe[4], C. Perrier[3], D. Queloz[4], and S. Udry[4]

[1] Departamento de Física, Universidade de Aveiro, Campus de Santiago, 3810-193 Aveiro, Portugal
e-mail: correia@ua.pt
[2] IMCCE, CNRS-UMR8028, Observatoire de Paris, UPMC, 77 avenue Denfert-Rochereau, 75014 Paris, France
[3] Laboratoire d'Astrophysique, Observatoire de Grenoble, Université J. Fourier, CNRS-UMR5571, BP 53, 38041 Grenoble, France
[4] Observatoire de Genève, Université de Genève, 51 ch. des Maillettes, 1290 Sauverny, Switzerland
[5] Service d'Aéronomie du CNRS/IPSL, Université de Versailles Saint-Quentin, BP 3, 91371 Verrières-le-Buisson, France
[6] Institut d'Astrophysique de Paris, CNRS, Université Pierre et Marie Curie, 98 bis Bd Arago, 75014 Paris, France

Received 15 June 2009 / Accepted 6 October 2009

ABSTRACT

Precise radial-velocity measurements for data acquired with the HARPS spectrograph infer that three planets orbit the M 4 dwarf star GJ 876. In particular, we confirm the existence of planet *d*, which orbits every 1.93785 days. We find that its orbit may have significant eccentricity ($e = 0.14$), and deduce a more accurate estimate of its minimum mass of 6.3 $M_\oplus$. Dynamical modeling of the HARPS measurements combined with literature velocities from the Keck Observatory strongly constrain the orbital inclinations of the *b* and *c* planets. We find that $i_b = 48.9° \pm 1.0°$ and $i_c = 48.1° \pm 2.1°$, which infers the true planet masses of $M_b = 2.64 \pm 0.04\ M_{\rm Jup}$ and $M_c = 0.83 \pm 0.03\ M_{\rm Jup}$, respectively. Radial velocities alone, in this favorable case, can therefore fully determine the orbital architecture of a multi-planet system, without the input from astrometry or transits.
The orbits of the two giant planets are nearly coplanar, and their 2:1 mean motion resonance ensures stability over at least 5 Gyr. The libration amplitude is smaller than 2°, suggesting that it was damped by some dissipative process during planet formation. The system has space for a stable fourth planet in a 4:1 mean motion resonance with planet *b*, with a period around 15 days. The radial velocity measurements constrain the mass of this possible additional planet to be at most that of the Earth.

Key words. stars: individual: GJ 876 – planetary systems – techniques: radial velocities – methods: observational – methods: numerical – celestial mechanics

1. Introduction

Also known as IL Aqr, GJ 876 is only 4.72 pc away from our Sun and is thus the closest star known to harbor a multi-planet system. It has been tracked by several instruments and telescopes from the very beginning of the planetary hunt in 1994, namely the Hamilton (Lick), HIRES (Keck) echelle spectrometers, ELODIE (Haute-Provence), and CORALIE (La Silla) spectrographs. More recently, it was also included in the HARPS program.

The *HARPS search for southern extra-solar planets* is an extensive radial-velocity survey of some 2000 stars in the solar neighborhood conducted with the HARPS spectrograph on the ESO 3.6-m telescope at La Silla (Chile) in the framework of Guaranteed Time Observations granted to the HARPS building consortium (Mayor et al. 2003). About 10% of the HARPS GTO time were dedicated to observe a volume-limited sample of ~110 M dwarfs. This program has proven to be very efficient in finding Neptunes (Bonfils et al. 2005b, 2007) and Super-Earths (Udry et al. 2007; Forveille et al. 2009; Mayor et al. 2009) down to $m \sin i = 1.9\ M_\oplus$. Because M dwarfs are more favorable targets to searches for lower mass and/or cooler planets than around Sun-like stars, the observational effort dedicated by ESO has increased by a factor of four, to an extended sample of 300 stars.

The first planet around GJ 876, a Jupiter-mass planet with a period of about 61 days, was simultaneous reported by Delfosse et al. (1998) and Marcy et al. (1998). Later, Marcy et al. (2001) found that the 61-day signal was produced by two planets in a 2:1 mean motion resonance, the inner one with 30-day period also being a gas giant. While investigating the dynamical interactions between those two planets, Rivera et al. (2005) found evidence of a third planet, with an orbital period less than 2 days and a minimum mass of 5.9 $M_\oplus$, which at that time was the lowest mass detected companion to a main-sequence star other than the Sun.

Systems with two or more interacting planets dramatically improve our ability to understand planetary formation and evolution, since dynamical analysis can both constrain their evolutionary history and more accurately determine their orbital "structure". Amongst known multi-planet systems, planets GJ 876 *b* and *c* have by far the strongest mutual gravitational interactions,

⋆ Based on observations made with the HARPS instrument on the ESO 3.6 m telescope at La Silla Observatory under the GTO programme ID 072.C-0488; and on observations obtained at the Keck Observatory, which is operated jointly by the University of California and the California Institute of Technology.

⋆⋆ The Table with the HARPS radial velocities is only available in electronic form at the CDS via anonymous ftp to cdsarc.u-strasbg.fr (130.79.128.5) or via http://cdsweb.u-strasbg.fr/cgi-bin/qcat?J/A+A/511/A21

and all their orbital quantities change quite rapidly. Since the radial velocity of GJ 876 has been monitored for the past 15 years, the true masses of these two planets can be determined by adjusting the inclination of their orbital planes when fitting dynamical orbits to the observational data. This was first attempted by Rivera & Lissauer (2001), who found a broad minimum in the residuals to the observed radial velocities for inclinations higher than 30°, the best-fit function corresponding to ~37°. Astrometric observations of GJ 876 with the *Hubble Space Telescope* subsequently suggested a higher value of ~85° (Benedict et al. 2002). Rivera et al. (2005) re-examined the dynamical interactions with many additional Keck radial velocity measurements, and found an intermediate inclination of ~50°. Bean & Seifahrt (2009) reconciled the astrometry and radial velocities by performing a joint adjustment to the Keck and HST datasets, and showed that both are consistent with ~50°. Early inclination determinations were, in retrospect, affected by small-number statistics (for astrometry) and by a modest signal-to-noise ratio in the radial velocity residuals.

In the present study, we reanalyze the GJ 876 system, including 52 additional high precision radial velocity measurements taken with the HARPS spectrograph. We confirm the presence of a small planet *d* and determine the masses of *b* and *c* with great precision. Section 2 summarizes information about the GJ 876 star. Its derived orbital solution is described in Sect. 3, and the dynamical analysis of the system is discussed in Sect. 4. Finally, conclusions are drawn in Sect. 5.

2. Stellar characteristics of GJ 876

GJ 876 (IL Aquarii, Ross 780, HIP 113020) is a M 4 dwarf (Hawley et al. 1996) in the Aquarius constellation. At 4.7 pc ($\pi = 212.69 \pm 2.10$ mas – ESA 1997), it is the 41st closest known stellar system[1] and only the 3rd closest known planetary system (after ϵ Eridani, and slightly further away than GJ 674).

Its photometry ($V = 10.162 \pm 0.009$, $K = 5.010 \pm 0.021$ – Turon et al. 1993; Cutri et al. 2003) and its parallax imply absolute magnitudes of $M_V = 11.80 \pm 0.05$ and $M_K = 6.65 \pm 0.05$. The $J-K$ color of GJ 876 (=0.92 – Cutri et al. 2003) and the Leggett et al. (2001) color-bolometric relation infer a K-band bolometric correction of $BC_K = 2.80$, and a 0.013 $L_\odot$ luminosity. The K-band mass-luminosity relation of Delfosse et al. (2000) implies a 0.334 $M_\odot$ mass, which is comparable to the 0.32 $M_\odot$ derived by Rivera et al. (2005) from Henry & McCarthy (1993). Bonfils et al. (2005a) estimate it has an approximately solar metallicity ([Fe/H] = 0.02 ± 0.2). Johnson & Apps (2009) revised this metallicity calibration for the most metal-rich M dwarfs and found that GJ 876 has an above solar metallicity ([Fe/H] > +0.3 dex).

In terms of magnetic activity, GJ 876 is also an average star in our sample. Its Ca II H&K emission is almost twice the emission of Barnard's star, an old star in our sample of the same spectral type, but still comparable to many stars with low jitter (rms ~ 2 m s^{-1}). On the one hand, its long rotational period and magnetic activity imply an old age (>0.1 Gyr). On the other hand, its UVW Galactic velocities place GJ 876 in the young disk population (Leggett 1992), suggesting an age <5 Gyr, and therefore bracketing its age to ~0.1−5 Gyr.

Rivera et al. (2005) monitored GJ 876 for photometric variability and found a 96.7-day periodic variation with a ~1% amplitude, hence identifying the stellar rotation. This corresponds to a low rotational velocity ($v \sin i = 0.16$ km s^{-1}) that is particularly helpful for radial-velocity measurements as a dark spot covering 1% of GJ 876's surface and located on its equator would produce a Doppler modulation with a maximum semi-amplitude of only ~1.5 m s^{-1}.

Finally, the high proper motion of GJ 876 (1.17 arcsec yr^{-1} – ESA 1997) changes the orientation of its velocity vector along the line of sight (e.g. Kürster et al. 2003) resulting in an apparent secular acceleration of 0.15 m s^{-1} yr^{-1}. Before our orbital analysis, we removed this drift for both HARPS and already published data.

Table 1. Observed and inferred stellar parameters of GJ 876.

Parameter		GJ 876
Sp		M4 V
V	[mag]	10.162
π	[mas]	212.69 ± 2.10
M_V	[mag]	11.80 ± 0.05
[Fe/H]	[dex]	0.05 ± 0.20
L	[$L_\odot$]	0.013
M_*	[$M_\odot$]	0.334 ± 10%
$P_{\rm rot}$	[day]	96.7
$v \sin i$	[km s^{-1}]	0.16
age(log $R'_{\rm HK}$)	[Gyr]	0.1−5

3. Orbital solution for the GJ 876 system

3.1. Keck + HARPS

The HARPS observations of GJ 876 started in December 2003 and have continued for more than four years. During this time, we acquired 52 radial-velocity measurements with an average precision of 1.0 m s^{-1}.

Before the HARPS program, the star GJ 876 had already been followed since June 1997 by the HIRES spectrometer mounted on the 10-m telescope I at Keck Observatory (Hawaii). The last published set of data acquired at Keck are from December 2004 and correspond to 155 radial-velocity measurements with an average precision of 4.3 m s^{-1} (Rivera et al. 2005).

When combining the Keck and the HARPS data for GJ 876, the time span for the observations increases to more than 11 years, and the secular dynamics of the system can be far more tightly constrained, although the average precision of the Keck measurements is about four times less accurate than for HARPS.

3.2. Two planet solution

With 207 measurements (155 from Keck and 52 from HARPS), we are now able to determine the nature of the three bodies in the system with great accuracy. Using the iterative Levenberg-Marquardt method (Press et al. 1992), we first attempt to fit the complete set of radial velocities with a 3-body Newtonian model (two planets) assuming coplanar motion perpendicular to the plane of the sky, similarly to that achieved for the system HD 202206 (Correia et al. 2005). This fit yields the well-known planetary companions at $P_b = 61$ day, and $P_c = 30$ day, and an adjustment of $\sqrt{\chi^2} = 2.64$ and rms = 4.52 m s^{-1}.

3.3. Fitting the inclinations

Because of the proximity of the two planets and their high minimum masses, the gravitational interactions between these two

[1] http://www.chara.gsu.edu/RECONS/TOP100.posted.htm

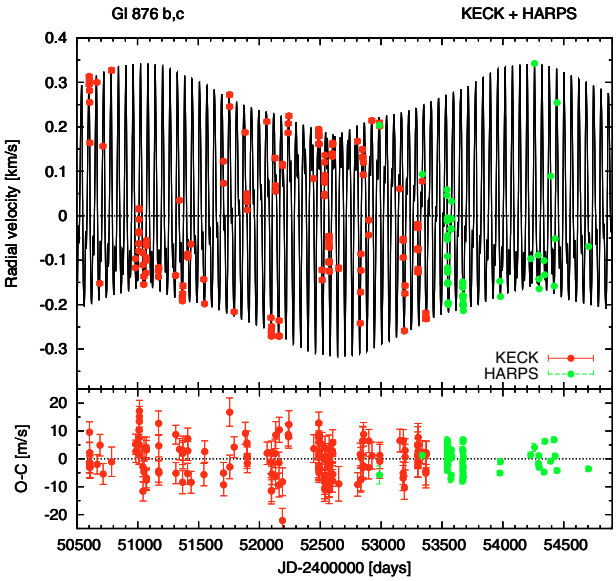

Fig. 1. Keck and HARPS radial velocities for GJ 876, superimposed on the 3-body Newtonian (two planets) orbital solution for planets b and c (orbital parameters taken from Table 2).

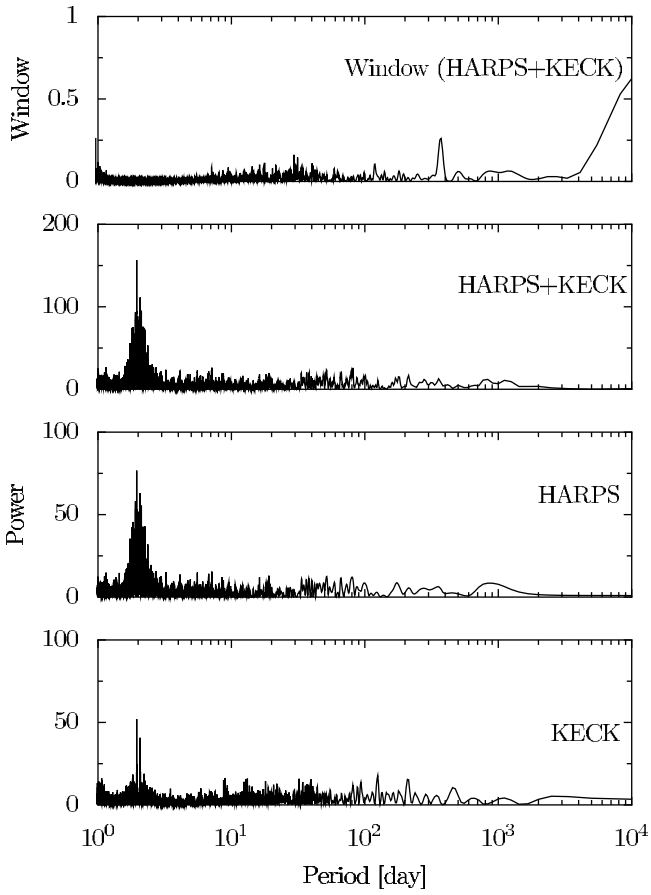

Fig. 2. Frequency analysis and window function for the two-planet Keck and HARPS residual radial velocities of GJ 876 (Fig. 1). An important peak is detected at $P = 1.9379$ day, which can be interpreted as a third planetary companion in the system. Looking at the window function, we can see that this peak is not an artifact.

bodies are strong. Since the observational data cover more than one decade, we can expect to constrain the inclination of their orbital planes. Without loss of generality, we use the plane of the sky as a reference plane, and choose the line of nodes of planet b as a reference direction in this plane ($\Omega_b = 0$). We thus add only three free parameters to our fit: the longitude of the node Ω_c of planet c, and the inclinations i_b and i_c of planets b and c with respect to the plane of the sky.

This fit yields $i_b = 57°$, $i_c = 63°$, and $\Omega_c = -1°$, and an adjustment of $\sqrt{\chi^2} = 2.57$ and rms $= 4.35$ m s^{-1}. Although there is no significant improvement to the fit, an important difference exists: the new orbital parameters for both planets show some deviations and, more importantly, the inclinations of both planets are well constrained. In Fig. 1, we plot the Keck and HARPS radial velocities for GJ 876, superimposed on the 3-body Newtonian orbital solution for planets b and c.

3.4. Third planet solution

The residuals around the best-fit two-planet solution are small, but still larger than the internal errors (Fig. 1). We may then search for other companions with different orbital periods. Performing a frequency analysis of the velocity residuals (Fig. 1), we find an important peak signature at $P = 1.9379$ day (Fig. 2). This peak was already present in the Keck data analysis performed by Rivera et al. (2005), but it is here reinforced by the HARPS data. In Fig. 2, we also plot the window function and conclude that the above mentioned peak cannot be an aliasing of the observational data.

To test the planetary nature of the signal, we performed a Keplerian fit to the residuals of the two planets. We found an elliptical orbit with $P_d = 1.9378$ day, $e_d = 0.14$, and $M_d \sin i_d = 5.4\ M_\oplus$. The adjustment gives $\sqrt{\chi^2} = 1.52$ and rms $= 2.63$ m s^{-1}, which represents a substantial improvement with respect to the system with only two companions (Fig. 1).

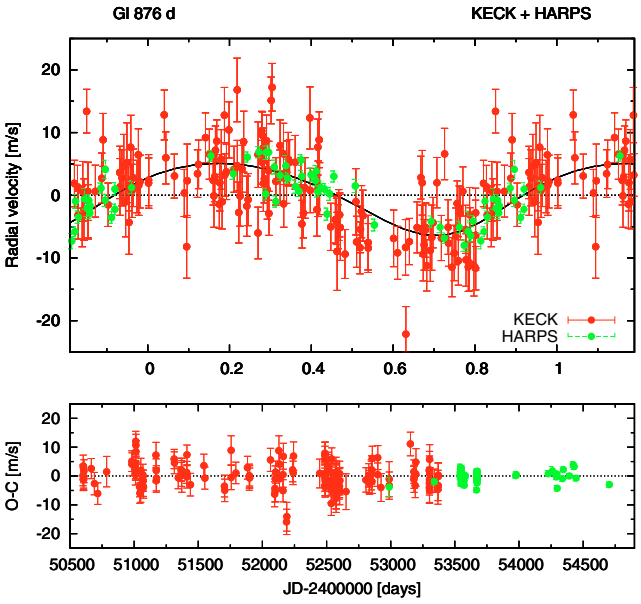

Fig. 3. Phase-folded residual radial velocities for GJ 876 when the contributions from the planets b and c are subtracted. Data are superimposed on a Keplerian orbit of $P = 1.9378$ day and $e = 0.14$ (the complete set of orbital parameters are those from Table 2). The respective residuals as a function of Julian date are displayed in the lower panel.

Table 2. Orbital parameters for the planets orbiting GJ 876, obtained with a 4-body Newtonian fit to observational data from Keck and HARPS.

Param.	[Unit]	b	c	d
Date	[JD]		2 455 000.00 (fixed)	
$V_{(\mathrm{Keck})}$	[km s^{-1}]		0.0130 ± 0.0004	
$V_{(\mathrm{HARPS})}$	[km s^{-1}]		−1.3388 ± 0.0004	
P	[day]	61.067 ± 0.011	30.258 ± 0.009	1.93785 ± 0.00002
λ	[deg]	35.61 ± 0.14	158.62 ± 0.80	29.94 ± 3.30
e		0.029 ± 0.001	0.266 ± 0.003	0.139 ± 0.032
ω	[deg]	275.52 ± 2.67	275.26 ± 1.25	170.60 ± 15.52
K	[m s^{-1}]	212.24 ± 0.33	86.15 ± 0.40	6.67 ± 0.26
i	[deg]	48.93 ± 0.97	48.07 ± 2.06	50 (fixed)
Ω	[deg]	0 (fixed)	−2.32 ± 0.94	0 (fixed)
$a_1 \sin i$	[10^{-3} AU]	1.19	0.23	1.2×10^{-3}
$f(M)$	[10^{-9} $M_\odot$]	60.41	1.79	5.8×10^{-5}
$M \sin i$	[$M_\oplus$]	–	–	6.3
M	[M_{Jup}]	2.64	0.83	–
a	[AU]	0.211	0.132	0.021
N_{meas}			207	
Span	[day]		4103	
$\sqrt{\chi^2}$			1.37	
$\mathrm{rms}_{(\mathrm{Keck})}$	[m s^{-1}]		4.25	
$\mathrm{rms}_{(\mathrm{HARPS})}$	[m s^{-1}]		1.80	

Notes. Errors are given by the standard deviation σ, and λ is the mean longitude of the date.

3.5. Complete orbital solution

Starting with the orbital parameters derived in the above sections, we can now consider the best-fit orbital solution for GJ 876. Using the iterative Levenberg-Marquardt method, we then fit the complete set of radial velocities with a 4-body Newtonian model. In this model, 20 parameters out of 23 possible are free to vary. The three fixed parameters are $\Omega_b = 0°$ (by definition of the reference plane), but also $\Omega_d = 0°$ and $i_d = 50°$, because the current precision and time span of the observations are not large enough to constrain these two orbital parameters. However, the quality of the fit does not change if we choose other values for these parameters.

The orbital parameters corresponding to the best-fit solution are listed in Table 2. In particular, we find $i_b = 48.9° \pm 1.0°$ and $i_c = 48.1° \pm 2.1°$, which infer, respectively, $M_b = 2.64 \pm 0.04\ M_{\mathrm{Jup}}$ and $M_c = 0.83 \pm 0.03\ M_{\mathrm{Jup}}$ for the true masses of the planets. This fit yields an adjustment of $\sqrt{\chi^2} = 1.37$ and rms $= 2.29$ m s^{-1}, which represents a significant improvement with respect to all previous solutions. We note that the predominant uncertainties are related to the star's mass (Table 1), but these are not folded into the quoted error bars.

The best-fit orbit for planet d is also eccentric, in contrast to previous determinations in which its value was constrained to be zero (Rivera et al. 2005; Bean & Seifahrt 2009). We can also fix this parameter and our revised solution corresponds to an adjustment with $\sqrt{\chi^2} = 1.40$ and rms $= 2.34$ m s^{-1}. These values are compatible with the best-fit solution in Table 2, so we cannot rule out the possibility that future observations will decrease the eccentricity of planet d to a value close to zero.

3.6. Inclination of planet d

With the presently available data, we were able to obtain with great accuracy the inclinations of planets b and c. However, this was not the case for planet d, whose inclination was held fixed at 50° in the best-fit solution (Table 2). We are still unable to determine the inclination of the innermost planet, because the gravitational interactions between this planet and the other two are not as strong as the mutual interactions between the two outermost planets.

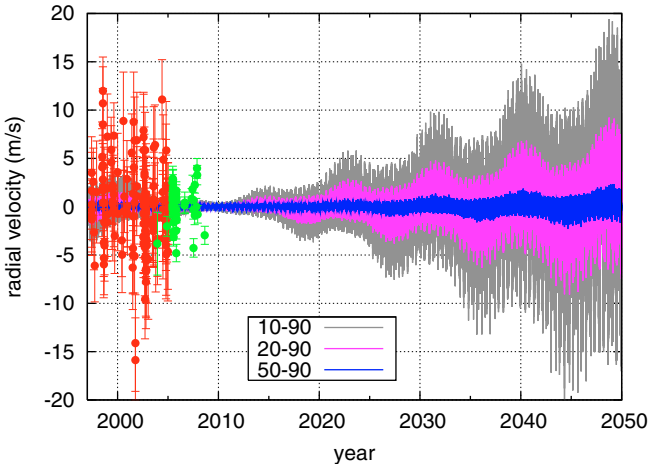

Fig. 4. Radial velocity differences between orbital solutions with i_d = 10°, 20°, and 50° and the orbital solution with $i_d = 90°$. We also plot the velocity residuals of the best-fit solution from Table 2. We observe that, with the current HARPS precision, the inclination will be constrained around 2025 if i_d is close to 10°, but if this planet is also coplanar with the other two ($i_d \sim 50°$), its precise value cannot be obtained before 2050.

We can nevertheless estimate the time span of GJ 876 radial velocity measures that is necessary before we will be able to determine the inclination i_d with good accuracy. For that purpose, we fit the observational data for different fixed values of the inclination of planet d (i_d = 10°, 20°, 50°, and 90°). In Fig. 4, we plot the evolution of the radial velocity differences between each solution and the solution at 90°. We also plot the velocity residuals of the best-fit solution from Table 2. We observe that, with the current HARPS precision, the inclination will be constrained around 2025 if i_d is close to 10°, but if this planet is also

coplanar with the other two ($i_d \sim 50°$), its precise value cannot be obtained before 2050 (Fig. 4).

3.7. Other instruments

Besides the Keck and HARPS programs, the star GJ 876 was also followed by many other instruments. The oldest observational data were acquired using the Hamilton echelle spectrometer mounted on the 3-m Shane telescope at the Lick Observatory. The star was followed from November 1994 until December 2000 and 16 radial velocity measurements were acquired with an average precision of 25 m s^{-1} (Marcy et al. 2001). During 1998, between July and September a quick series of 40 radial velocity observations were performed using the CORALIE echelle spectrograph mounted on the 1.2-m Swiss telescope at La Silla, with an average precision of 30 m s^{-1} (Delfosse et al. 1998). Finally, from October 1995 to October 2003, the star was also observed at the Haute-Provence Observatory (OHP, France) using the ELODIE high-precision fiber-fed echelle spectrograph mounted at the Cassegrain focus of the 1.93-m telescope. Forty-six radial velocity measurements were taken with an average precision of 18 m s^{-1} (data also provided with this paper via CDS).

We did not consider these data sets in the previous analysis because their inclusion would have been more distracting than profitable. Indeed, the internal errors of these three instruments are much higher than those from Keck and HARPS series, and they are unable to help in constraining the inclinations. Moreover, all the radial velocities are relative in nature, and therefore each data set included requires the addition of a free offset parameter in the orbit fitting procedure, $V_{\rm instrument}$.

Nevertheless, to be sure that there is no gain in including these additional 102 measurements, we performed an adjustment to the data using the five instruments simultaneously. The orbital parameters corresponding to the best-fit solution are listed in Table 3. As expected, this fit yields an adjustment of $\sqrt{\chi^2} = 1.46$ and rms = 3.01 ms^{-1}, which does not represent an improvement with respect to the fit listed in Table 2. The inclination of planet c decreases by 2.5°, but this difference is within the 3σ uncertainty of the best-fit values. Therefore, the orbital parameters determined only with data from Keck and HARPS will be adopted (Table 2).

4. Dynamical analysis

We now analyze the dynamics and stability of the planetary system given in Table 2. Because of the two outermost planets' proximity and high values of their masses, both planets are affected by strong planetary perturbations from each other. As a consequence, unless a resonant mechanism is present to avoid close encounters, the system cannot be stable.

4.1. Secular coupling

As usual in planetary systems, there is a strong coupling within the secular system (see Laskar 1990). Therefore, both planets b and c precess with the same precession frequency g_2, which is retrograde with a period of 8.74 years. The two periastron are thus locked and $\Delta\varpi = \varpi_c - \varpi_b$ oscillate around 0° with an amplitude of about 25° (Fig. 6). This behavior, already mentioned in earlier studies (Laughlin & Chambers 2001; Lee & Peale 2002; Beaugé et al. 2003), is not a dynamical resonance, but merely the result of the linear secular coupling. To present the solution in a clearer way, it is then useful to make a linear change of variables into eccentricity and inclination proper modes (see Laskar 1990). In the present case, the linear transformation is numerically obtained by a frequency analysis of the solutions. For the dynamical analysis, to understand the evolution of the inclinations in this system, we have expressed all the coordinates in the reference frame of the invariant plane, orthogonal to the total angular momentum of the system. The longitude of node Ω and inclination I of this invariant plane are

$$\Omega = -0.445256°; \quad I = 48.767266°. \tag{1}$$

Using the classical complex notation,

$$z_k = e_k e^{{\rm i}\varpi_k}; \quad \zeta_k = \sin(i_k/2) e^{{\rm i}\Omega_k}; \tag{2}$$

for $k = b, c, d$, we have for the linear Laplace-Lagrange solution

$$\begin{pmatrix} z_d \\ z_c \\ z_b \end{pmatrix} = \begin{pmatrix} 0.139690 & 0.000843 & -0.001265 \\ -0.000069 & 0.265688 & -0.006501 \\ 0.000063 & 0.037609 & 0.006970 \end{pmatrix} \begin{pmatrix} u_1 \\ u_2 \\ u_3 \end{pmatrix}, \tag{3}$$

where the proper modes u_k are obtained from the z_k by inverting the above linear relation. To good approximation, we then have $u_k \approx e^{{\rm i}(g_k t + \phi_k)}$, where g_k and ϕ_k are given in Table 4. For the inclinations, due to the conservation of the angular momentum, there are only two proper modes, v_1, v_2, which we can define with the invertible linear relation

$$\begin{pmatrix} \zeta_d \\ \zeta_c \end{pmatrix} = \begin{pmatrix} 0.009449 & +0.002723 \\ -0.000004 & -0.013783 \end{pmatrix} \begin{pmatrix} v_1 \\ v_2 \end{pmatrix}, \tag{4}$$

and the additional approximate relation

$$\zeta_b \approx -0.000028\, v_1 + 0.003301\, v_2. \tag{5}$$

The proper modes in inclination are then given to a good approximation as $v_k \approx e^{{\rm i}(s_k t + \psi_k)}$, where s_k and ψ_k are given in Table 4.

With Eq. (3), it is then easy to understand the meaning of the observed libration between the periastrons ϖ_b and ϖ_c. Indeed, for both planets b and c, the dominant term is the u_2 term with frequency g_2. They thus both precess with an average value of g_2. In the same way, both nodes Ω_b and Ω_c precess with the same frequency s_2. It should also be noted that Eqs. (3)–(5) provide good approximations of the long-term evolution of the eccentricities and inclinations. Indeed, in Fig. 5 we plot the eccentricity and the inclination with respect to the invariant plane of planets b, c, d, with initial conditions from Table 2. At the same time, we plot with solid black lines the evolution of the same elements given by the above secular, linear approximation.

The eccentricity and inclination variations are very limited and described well by the secular approximation. The eccentricity of planets b and c are within the ranges $0.028 < e_b < 0.050$ and $0.258 < e_c < 0.279$, respectively. These variations are driven mostly by the rapid secular frequency $g_3 - g_2$, of period $2\pi/(g_3 - g_2) \approx 8.62$ yr (Table 4). The eccentricity of planet d is nearly constant with $0.136 < e_d < 0.142$.

The inclinations of b and c with respect to the invariant plane are very small with $0.36° < i_b < 0.39°$ and $1.54° < i_c < 1.61°$, respectively. This small variation is mostly caused by the nonlinear secular term $2(s_2 - g_2)$ of period 4.791 yr. Although the inclination of d is not well constrained, using the initial conditions of Table 2, one finds small variations in its inclination $0.76° < i_d < 1.42°$, which are driven by the secular frequency $s_1 - s_2$ of period 138.3 yr (Table 4).

With the present 11 years of observations covered by Keck and HARPS, the most important features that allow us to constrain the parameters of the system are those related to the rapid secular frequencies g_2 and s_2, of periods 8.7 yr and 99 yr, which are the precession frequencies of the periastrons and nodes of planets b and c.

Table 3. Orbital parameters for the planets orbiting GJ 876, obtained with a 4-body Newtonian fit to all available radial velocity observational data (Lick, Keck, CORALIE, ELODIE, and HARPS).

Param.	[Unit]	b	c	d
Date	[JD]		2 455 000.00 (fixed)	
$V_{\rm Lick}$	[km s^{-1}]		-0.0304 ± 0.0058	
$V_{\rm Keck}$	[km s^{-1}]		0.0131 ± 0.0058	
$V_{\rm CORALIE}$	[km s^{-1}]		-1.8990 ± 0.0061	
$V_{\rm ELODIE}$	[km s^{-1}]		-1.8624 ± 0.0064	
$V_{\rm HARPS}$	[km s^{-1}]		-1.3389 ± 0.0058	
P	[day]	61.065 ± 0.012	30.259 ± 0.010	1.93785 ± 0.00002
λ	[deg]	35.56 ± 0.15	159.05 ± 0.76	29.37 ± 3.21
e		0.031 ± 0.001	0.265 ± 0.002	0.124 ± 0.032
ω	[deg]	274.69 ± 2.57	274.64 ± 1.19	168.45 ± 17.21
K	[m s^{-1}]	212.09 ± 0.33	85.91 ± 0.40	6.60 ± 0.26
i	[deg]	48.98 ± 0.94	45.67 ± 1.81	50 (fixed)
Ω	[deg]	0 (fixed)	-1.67 ± 0.84	0 (fixed)
$a_1 \sin i$	[10^{-3} AU]	1.19	0.23	1.2×10^{-3}
$f(M)$	[10^{-9} $M_\odot$]	60.27	1.78	5.6×10^{-5}
$M \sin i$	[$M_\oplus$]	–	–	6.2
M	[$M_{\rm Jup}$]	2.64	0.86	–
a	[AU]	0.211	0.132	0.021
$N_{\rm meas}$			309	
Span	[day]		5025	
$\sqrt{\chi^2}$			1.46	
rms	[m s^{-1}]		3.01	

Notes. Errors are given by the standard deviation σ, and λ is the mean longitude of the date.

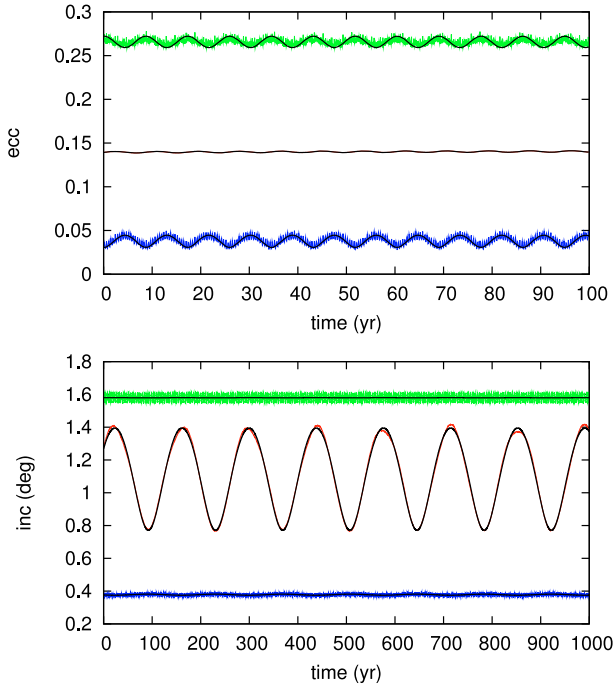

Fig. 5. Evolution of the GJ 876 eccentricities (*top*) and inclinations (*bottom*) with time, starting with the orbital solution from Table 2. The color lines are the complete solutions for the various planets (b: blue, c: green, d: red), while the black curves are the associated values obtained with the linear, secular model.

Table 4. Fundamental frequencies and phases for the orbital solution in Table 2.

	Frequency deg/yr	Period yr		Phase deg
n_b	2154.322532	0.167106	λ_{b0}	36.0925
n_c	4349.841605	0.082762	λ_{c0}	158.1879
n_d	67852.886097	0.005306	λ_{d0}	29.6886
g_1	1.003492	358.747259	ϕ_1	170.0005
g_2	–41.196550	8.738596	ϕ_2	-86.0030
g_3	0.555047	648.593233	ϕ_3	89.8880
s_1	–1.021110	352.557387	ψ_1	3.9446
s_2	–3.624680	99.319103	ψ_2	64.1066
l_θ	245.918001	1.463903	θ_0	-48.6812

Notes. n_b, n_c and n_d are the mean motions, g_1, g_2 and g_3 the main secular frequencies of the periastrons, s_1 and s_2 the main secular frequencies of the nodes, and l_θ the libration frequency of the resonant angles.

4.2. The 2:1 mean motion resonance

The ratio of the orbital periods of the two outermost planets determined by the fitting process (Table 2) is $P_b/P_c = 2.018$, suggesting that the system may be trapped in a 2:1 mean motion resonance. This resonant motion has already been reported in previous works (Laughlin & Chambers 2001; Rivera & Lissauer 2001; Lee & Peale 2002; Ji et al. 2002; Rivera et al. 2005). To test the accuracy of this scenario, we performed a frequency analysis of the orbital solution listed in Table 2 computed over 100 kyr. The orbits of the three planets are integrated with the symplectic integrator SABA4 of Laskar & Robutel (2001), using a step size of 2×10^{-4} years. We conclude that in the nominal solution of Table 2, planets b and c in the GJ 876 system indeed show a 2:1 mean motion resonance, with resonant arguments: $\theta_b = 2\lambda_b - \lambda_c - \varpi_b$ and $\theta_c = 2\lambda_b - \lambda_c - \varpi_c$.

If we analyze these arguments, it is indeed difficult to disentangle the proper libration from the secular oscillation of the periastrons angles ϖ_b, ϖ_c. It is thus much clearer to switch to

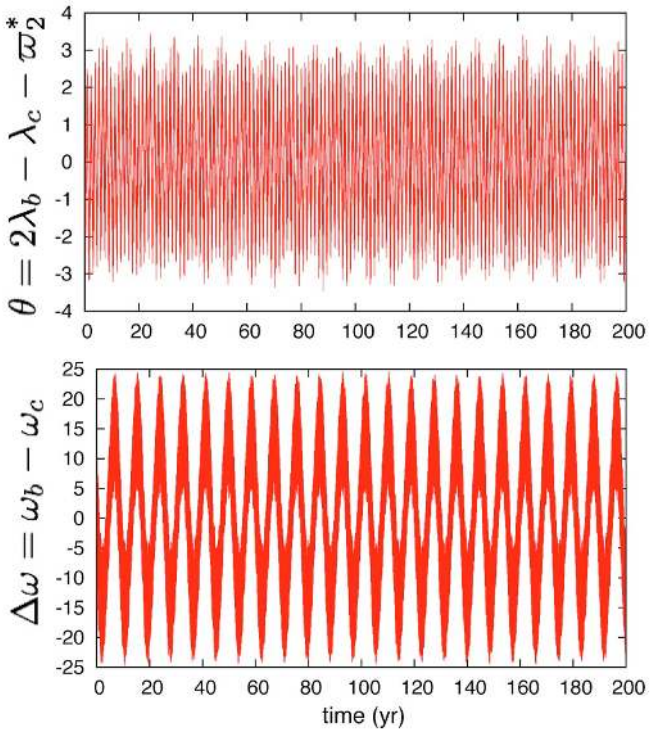

Fig. 6. Variation in the resonant argument $\theta = 2\lambda_b - \lambda_c - \varpi_2^*$ with time (top). The difference $\Delta\omega = \varpi_b - \varpi_c$ also oscillates around 0° with a 25° amplitude.

Table 5. Quasi-periodic decomposition of the resonant angle $\theta = 2\lambda_b - \lambda_c - \varpi_2^*$ for an integration over 100 kyr of the orbital solution in Table 2.

Combination					ν_i	A_i	ϕ_i
n_b	n_c	g_2	g_3	l_θ	(deg/yr)	(deg)	(deg)
0	0	0	0	1	245.9180	1.810	–48.681
1	1	–2	0	0	6586.5572	0.567	96.286
0	1	–1	0	0	2195.5191	0.569	32.095
0	0	–1	1	0	41.7516	0.411	–94.109
1	0	–1	0	0	4391.0382	0.255	–25.809
2	1	–3	0	0	10977.5954	0.156	–19.523
0	0	1	-1	1	204.1664	0.120	–44.572

Notes. We have $\theta = \sum_{i=1}^{N} A_i \cos(\nu_i\, t + \phi_i)$. We only provide the first 7 largest terms that are identified as integer combinations of the fundamental frequencies given in Table 4.

proper modes u_k, v_k by means of the linear transformation (3, 4). Indeed, if $u_k = e^{i\varpi_k^*}$, the argument

$$\theta = 2\lambda_b - \lambda_c + \varpi_2^* \tag{6}$$

is in libration around 0° with a very small total amplitude of 3.5° (Fig. 6) with only 1.8° amplitude related to the proper libration argument θ with period $2\pi/l_\theta = 1.46$ yr. The remaining terms of Table 5 are forced terms related to planetary interactions. The fundamental frequencies associated with this libration argument (Table 4) indeed verify the resonance relation $2n_b - n_c - g_2 = 0$ up to the precision of the determination of the frequencies ($\approx 10^{-5}$).

4.3. Coplanar motion

The orbits of the planets in the Solar System are nearly coplanar, that is, their orbital planes remain within a few degrees of inclination from an inertial plane perpendicular to the total angular momentum of the system. The highest inclination is obtained for Mercury ($I \sim 7°$), which is also the smallest of the eight planets.

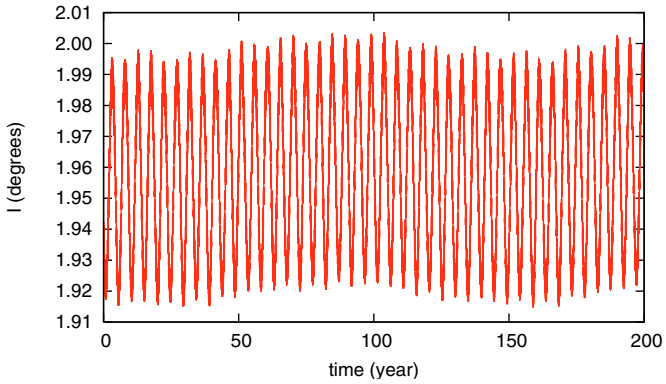

Fig. 7. Evolution of the mutual inclination of the planets b and c. Since the maximal inclination between the two planets is 2.0°, we conclude that the orbits are almost coplanar, as in our Solar System.

A general belief that planetary systems would tend to resemble the Solar System persists, but there is no particular reason for all planetary systems to be coplanar such as our own. Star formation theories require an accretion disk in which planets form, but close encounters during the formation process can increase the eccentricities and inclinations (e.g. Lee et al. 2007). That planets are found to have significant eccentricity values is also consistent with their having high inclinations (e.g. Libert & Tsiganis 2009). In particular, studies of Kuiper belt objects indicate that there is an important inclination excitation when the bodies sweep secular resonances (e.g. Nagasawa et al. 2000; Li et al. 2008), a mechanism that also appears to be applicable to planets (e.g. Thommes & Lissauer 2003).

The question of whether extra-solar planetary systems are also nearly coplanar or not is thus important. Although about 45 extra-solar multi-planet systems have been reported, their true inclinations have so far been determined in only two cases. One is the planetary system around the pulsar PSR B1257 + 12, discovered by precise timing measurements of pulses (Wolszczan & Frail 1992), for which the orbits seem to be almost coplanar (Konacki & Wolszczan 2003). The other case is GJ 876, the only planetary system around a main-sequence star for which one can access the inclinations. This result is possible because of the large amount of data already available and because the two giant planets show strong gravitational interactions.

The analytical expressions and the plots versus time of the orbital elements in the reference frame of the invariant plane show that the inclinations of planets b and c are both very small (Eqs. (4), (5), Fig. 5). To test the coplanarity of this system, we plot in Fig. 7 the evolution of the mutual inclination with time. We verify that $I = 1.958° \pm 0.045°$, and hence conclude that the orbits of planets b and c are indeed nearly coplanar.

In our best-fit solution (Table 2), we also assumed that the orbit of planet d is nearly coplanar with the other two planets, but there is no clear physical reason that justifies our choice. Indeed, its orbit should be more perturbed by the oblateness of the star, rather than the other planets (Goldreich 1965; Correia 2009). It is therefore more likely that planet d orbits in the equatorial plane of the star. This plane can be identical to the orbital plane of the outer planets or not, depending on the evolutionary process. According to Fig. 2, with the current HARPS precision of $\sim$1 m s^{-1}, we will have to wait until about 2050 to confirm an inclination close to 50°.

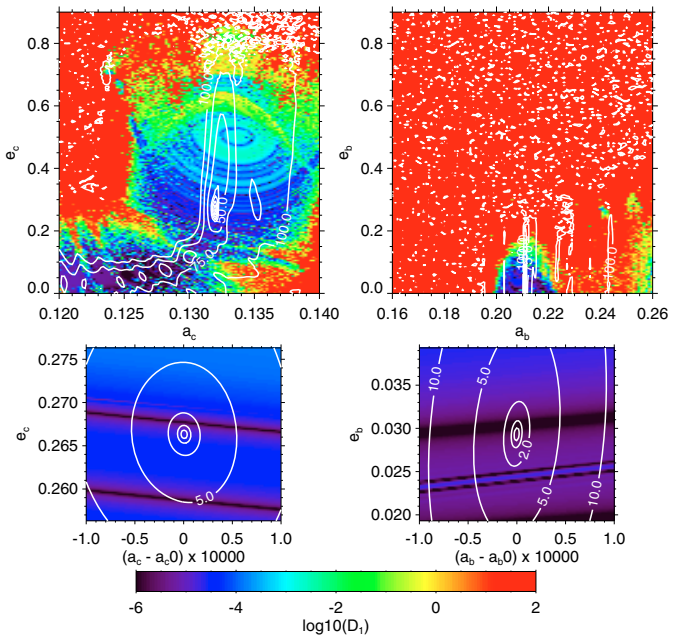

Fig. 8. Stability analysis of the nominal fit (Table 2) of the GJ 876 planetary system. For a fixed initial condition of planet b (*left*) and planet c (*right*), the phase space of the system is explored by varying the semi-major axis a_k and eccentricity e_k of the other planet, respectively. The step size is 0.0002 AU in semi-major axis and 0.005 in eccentricity in the top panels and 2×10^{-6} AU and 2×10^{-4} in *bottom panels*. For each initial condition, the system is integrated over 800 yr with an averaged model for planet d (Farago et al. 2009) and a stability criterion is derived with the frequency analysis of the mean longitude (Laskar 1990, 1993). As in Correia et al. (2005, 2009), the chaotic diffusion is measured by the variation in the frequencies. The "red" zone corresponds to highly unstable orbits, while the "dark blue" region can be assumed to be stable on a billion-years timescale. The contour curves indicate the value of χ^2 obtained for each choice of parameters. It is remarkable that in the present fit, there is an exact correspondence between the zone of minimal χ^2 and the 2:1 stable resonant zone, in "dark blue".

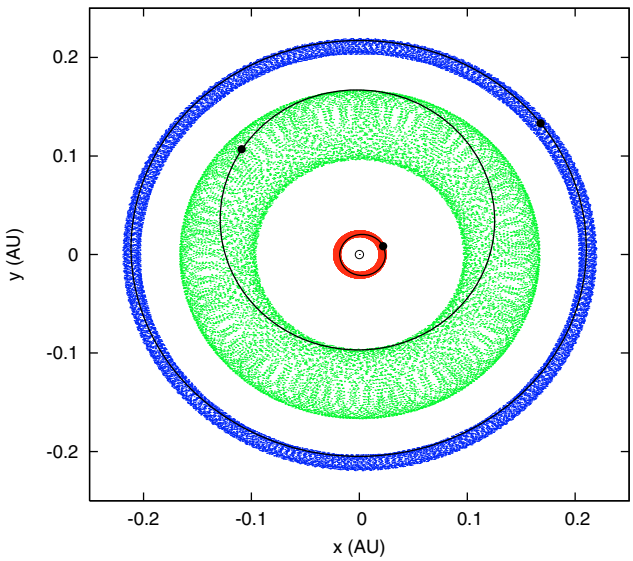

Fig. 9. Long-term evolution of the GJ 876 planetary system over 100 Myr starting with the orbital solution from Table 2. We did not include tidal effects in this simulation. The panel shows a face-on view of the system invariant plane. x and y are spatial coordinates in a frame centered on the star. Present orbital solutions are traced with solid lines and each dot corresponds to the position of the planet every 5 kyr. The semi-major axes (in AU) are almost constant ($0.209 < a_b < 0.214$; $0.131 < a_c < 0.133$ and $0.02110 < a_d < 0.02111$), and the eccentricities present slight variations ($0.028 < e_b < 0.050$; $0.258 < e_c < 0.279$ and $0.136 < e_d < 0.142$).

Adopting $\Omega_d = 0°$, and initial values of i_d ranging from 10° to 90°, we found best-fit solutions with very similar values of reduced $\sqrt{\chi^2}$ as the solution in Table 2. For inclinations lower than 10°, the best-fit solution becomes worse ($\sqrt{\chi^2} = 1.58$ for $i_d = 5°$) and infers low eccentricity values for planet d. In addition, planets b and c are no longer nearly coplanar. We therefore conclude that a lower limit to the inclination of planet d can be set to be around 10°. On the other hand, a lack of transit detections only allows inclinations close to 90° if the planet is very dense (Rivera et al. 2005).

4.4. Stability analysis

To analyze the stability of the nominal solution (Table 2) and confirm the presence of the 2:1 resonance, we performed a global frequency analysis (Laskar 1993) in the vicinity of this solution (Fig. 4), in the same way as achieved for the HD 45364 system by Correia et al. (2009).

For each planet, the system is integrated on a regular 2D mesh of initial conditions, with varying semi-major axis and eccentricity, while the other parameters are retained at their nominal values (Table 2). The solution is integrated over 800 yr for each initial condition and a stability indicator is computed to be the variation in the measured mean motion over the two consecutive 400 yr intervals of time. For regular motion, there is no significant variation in the mean motion along the trajectory, while it can vary significantly for chaotic trajectories. The result is reported in color in Fig. 8, where "red" represents the strongly chaotic trajectories, and "dark blue" the extremely stable ones. To decrease the computation time, we averaged the orbit of planet d over its mean-motion and periastron, following Farago et al. (2009).

In the two top plots (Figs. 8a,b), the only stable zone that exists in the vicinity of the nominal solution corresponds to the stable 2:1 resonant areas. As for HD 45364 (Correia et al. 2009) and HD 60532 (Laskar & Correia 2009) planetary systems, there is a perfect coincidence between the stable 2:1 resonant islands, and curves of minimal χ^2 obtained by comparison with the observations. Since these islands are the only stable zones in the vicinity, this picture presents a very coherent view of dynamical analysis and radial velocity measurements, which reinforces the confidence that the present system is in a 2:1 resonant state.

The scale of the two bottom panels shows the remarkable precision of the data in light of the dynamical environment of the system. The darker structures in these plots can be identified as secondary resonances. For instance, in the bottom left plot of Fig. 7, the two dark horizontal lines starting at $e_c \simeq 0.269$ and 0.260 correspond, respectively, to $l_\theta + 6g_2 - 6g_3 + s_1 - s_2$ and $l_\theta + 6g_2 - 2g_3 - 4s_2$. We can also barely see the secondary resonance $l_\theta + 6g_2 - 6g_3$ just above the former one. In the bottom right plot, the bluer line starting at $e_b \simeq 0.023$ corresponds to $l_\theta + 6g_2 - 4g_3 - 2s_2$. A longer integration time would most probably provide more details about the resonant and secular dynamics.

4.5. Long-term orbital evolution

From the previous stability analysis, it is clear that planets b and c listed in Table 2 are trapped in a 2:1 mean motion resonance

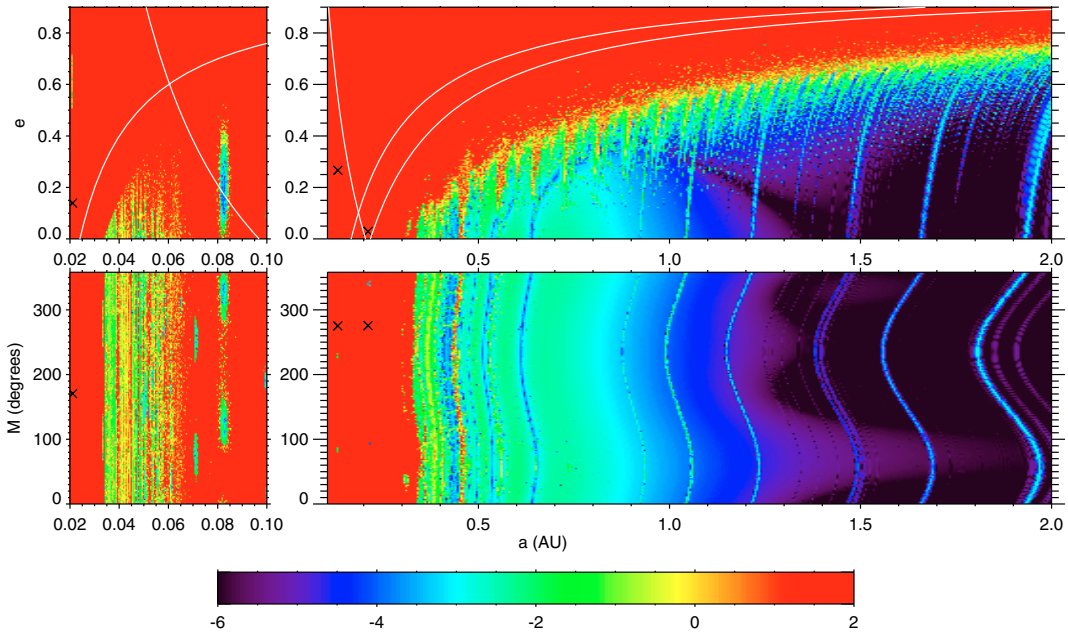

Fig. 10. Possible location of an additional fourth planet in the GJ 876 system. The stability of an Earth-size planet ($K = 1$ m s^{-1}) is analyzed, for various semi-major axis versus eccentricity (*top*), or mean anomaly (*bottom*). All the angles of the putative planets are set to 0° (except the mean anomaly in the bottom panels), its inclination to 50°, and in the bottom panels, its eccentricity to 0. The stable zones where additional planets can be found are the dark blue regions. Between the already known planets, we can find stability in a small zone corresponding to a 4:1 mean motion resonance with planet *b* (and 2:1 resonance with planet *c*). White lines represent the collisions with the already existing planets, given by a cross.

and stable over a Gyr timescale. Nevertheless, we also tested this by performing a numerical integration of the orbits using the symplectic integrator SABA4.

Because the orbital period of the innermost planet is shorter than 2 day, we performed two kinds of experiments. In the first one, we directly integrated the full planetary system over 100 Myr with a step size of 2×10^{-4} years. Although tidal effects may play an important role in this system evolution, we did not include them. The result is displayed in Fig. 9, showing that the orbits indeed evolve in a regular way, and remain stable throughout the simulation. For longer timescales, we needed to average the orbit of the inner planet as explained in Farago et al. (2009). We then use a longer step size of 2×10^{-3} years and integrated the system over 5 Gyr, which corresponds to the maximal estimated age of the central star. The subsystem consisting of the giant planets *b* and *c* remained stable.

In spite of the strong gravitational interactions between the two planets locked in the 2:1 mean motion resonance, both orbital eccentricities and inclinations exhibit small variations that are mostly driven by the regular linear secular terms (Fig. 5). These variations occur far more rapidly than in our Solar System, which enabled their direct detection using only 11 yr of data taken with Keck and HARPS together. It is important to notice, however, that for initial inclinations of planet *d* very different from 50°, the orbital perturbations from the outer planets may become important. For instance, using an orbital solution with $i_d = 90°$, we derive an eccentricity and inclination variations of $0.10 < e_d < 0.35$ and $10° < i_d < 90°$.

4.6. Additional constraints

The stability analysis summarized in Fig. 8 shows good agreement between the 2:1 resonant islands and the χ^2 contour curves. We can thus assume that the dynamics of the two known planets is not disturbed much by the presence of an additional planet close-by. The same is true for the innermost planet, which has an orbital period of 2 day, since the gravitational interaction with the parent star is too strong to be destabilized.

We then tested the possibility of an additional fourth planet in the system by varying the semi-major axis, the eccentricity, and the longitude of the periastron over a wide range, and performing a stability analysis (Fig. 10). The test was completed for a fixed value $K = 1$ m s^{-1}, corresponding to an Earth-size object. We also performed a simulation of a Neptune-size object ($K = 10$ m s^{-1}) without significant changes in its dynamics. In this last case, however, an object of this size would have already been detected in the data.

From this analysis (Fig. 10), one can see that stable orbits are possible beyond 1 AU and, very interestingly, also for orbital periods around 15 days (~0.083 AU), which correspond to bodies trapped in a 4:1 mean motion resonance with planet *b* (and 2:1 resonance with planet *c*). Between the already known planets, this is the only zone where additional planetary mass companions can survive. With the current HARPS precision of ~1 m s^{-1}, we estimate that any object with a minimum mass $M > 2\ M_\oplus$ would already be visible in the data. Since this does not seem to be the case, if we assume that a planet exists in this resonant stable zone, it should be an object smaller or not much larger than the Earth.

The presence of this fourth planet, not only fills an empty gap in the system, but can also help us to explain the anomalous high eccentricity of planet *d* ($e_d \sim 0.14$). Indeed, tidal interactions with the star should have circularized the orbit in less than 1 Myr, but according to Mardling (2007), the presence of an Earth-sized outer planet may delay the tidal damping of the eccentricity.

We propose that additional observational efforts should be made to search for this planet. The orbital period of only 15 day does not require long time of telescope and a planet with the mass of the Earth is at reach with the present resolution. Moreover, assuming coplanar motion with the outermost

planets, we obtain the exact mass for this planet and not a minimal estimation. We have reanalyzed the residuals of the system (Fig. 3), but so far no signal around 15 days appears to be present with the current precision. However, since this planet will be in a 2:1 mean motion resonance with planet *c*, we cannot exclude that the signal is hidden in the eccentricity of the giant planet (Anglada-Escude et al. 2010).

5. Discussion and conclusion

We have reanalyzed the planetary system orbiting the star GJ 876, using the new high-precision observational data acquired with HARPS. Independently from previous observations with other instruments, we can confirm the presence of planet *d*, orbiting at 1.93785 days, but in an elliptical orbit with an eccentricity of 0.14 and a minimum mass of 6.3 $M_{\oplus}$.

By combining the HARPS data with the data previously taken at the Keck Observatory, we are able to fully characterize the *b* and *c* planets. We find $i_b = 48.9° \pm 1.0°$ and $i_c = 48.1° \pm 2.1°$, which infers for the true masses of the planets $M_b = 2.64\ M_{\rm Jup}$ and $M_c = 0.83\ M_{\rm Jup}$, respectively. We hence conclude that the orbits of these two planets are nearly coplanar. The gravitational interactions between the outer planets and the innermost planet *d* may also allow us to determine its orbit more accurately in the near future. With the current precision of HARPS of $\sim$1 m s^{-1} for GJ 876, we expect to detect the true inclination and mass of planet *d* within some decades.

A dynamical analysis of this planetary system confirms that planets *b* and *c* are locked in a 2:1 mean motion resonance, which ensures stability over 5 Gyr. In the nominal solution, the resonant angles $\theta_b = 2\lambda_b - \lambda_c + \varpi_b$ and $\theta_c = 2\lambda_b - \lambda_c + \varpi_c$ are in libration around 0°, which means that their periastrons are also aligned. This orbital configuration may have been reached by means of the dissipative process of planet migration during the early stages of the system evolution (e.g. Crida et al. 2008). By analyzing the proper modes, we are able to see that the amplitude libration of the proper resonant argument $\theta = 2\lambda_b - \lambda_c + \varpi_2^*$ can be as small as 3.5°, of which only 1.8° is related to the libration frequency. It is thus remarkable that the libration amplitude is so small, owing to the width of the stable resonant island being large. We can thus assume that the libration amplitude has been damped by some dissipative process. This singular planetary system may then provide important constraints on planetary formation and migration scenarios.

Finally, we have found that stability is possible for an Earth-size mass planet or smaller in an orbit around 15 days, which is in a 4:1 mean motion resonance with planet *b*. The presence of this fourth planet, not only fills an empty gap in the system, but can also help us to explain the anomalous high eccentricity of planet *d* ($e_d \sim 0.14$), which should have been damped to zero by tides. Because of the proximity and low mass of the star, a planet with the mass of the Earth should be detectable at the present HARPS resolution.

We conclude that the radial-velocity technique is self sufficient for fully characterizing and determining all the orbital parameters of a multi-planet system, without needing to use astrometry or transits.

Acknowledgements. We acknowledge support from the Swiss National Research Found (FNRS), the Geneva University and French CNRS. A.C. also benefited from a grant by the Fundação para a Ciência e a Tecnologia, Portugal (PTDC/CTE-AST/098528/2008).

References

Anglada-Escude, G., Lopez-Morales, M., & Chambers, J. E. 2010, ApJ, 709, 168
Bean, J. L., & Seifahrt, A. 2009, A&A, 496, 249
Beaugé, C., Ferraz-Mello, S., & Michtchenko, T. A. 2003, ApJ, 593, 1124
Benedict, G. F., McArthur, B. E., Forveille, T., et al. 2002, ApJ, 581, L115
Bonfils, X., Delfosse, X., Udry, S., et al. 2005a, A&A, 442, 635
Bonfils, X., Forveille, T., Delfosse, X., et al. 2005b, A&A, 443, L15
Bonfils, X., Mayor, M., Delfosse, X., et al. 2007, A&A, 474, 293
Correia, A. C. M. 2009, ApJ, 704, L1
Correia, A. C. M., Udry, S., Mayor, M., et al. 2005, A&A, 440, 751
Correia, A. C. M., Udry, S., Mayor, M., et al. 2009, A&A, 496, 521
Crida, A., Sándor, Z., & Kley, W. 2008, A&A, 483, 325
Cutri, R. M., Skrutskie, M. F., van Dyk, S., et al. 2003, 2MASS All Sky Catalog of point sources, The IRSA 2MASS All-Sky Point Source Catalog, NASA/IPAC Infrared Science Archive http://irsa.ipac.caltech.edu/applications/Gator/
Delfosse, X., Forveille, T., Mayor, M., et al. 1998, A&A, 338, L67
Delfosse, X., Forveille, T., Ségransan, D., et al. 2000, A&A, 364, 217
ESA 1997, VizieR Online Data Catalog, 1239
Farago, F., Laskar, J., & Couetdic, J. 2009, Celestial Mechanics and Dynamical Astronomy, 104, 291
Forveille, T., Bonfils, X., Delfosse, X., et al. 2009, A&A, 493, 645
Goldreich, P. 1965, AJ, 70, 5
Hawley, S. L., Gizis, J. E., & Reid, I. N. 1996, AJ, 112, 2799
Henry, T. J., & McCarthy, Jr., D. W. 1993, AJ, 106, 773
Ji, J., Li, G., & Liu, L. 2002, ApJ, 572, 1041
Johnson, J. A., & Apps, K. 2009, ApJ, 699, 933
Konacki, M., & Wolszczan, A. 2003, ApJ, 591, L147
Kürster, M., Endl, M., Rouesnel, F., et al. 2003, A&A, 403, 1077
Laskar, J. 1990, Icarus, 88, 266
Laskar, J. 1993, Physica D Nonlinear Phenomena, 67, 257
Laskar, J., & Correia, A. C. M. 2009, A&A, 496, L5
Laskar, J., & Robutel, P. 2001, Celestial Mechanics and Dynamical Astronomy, 80, 39
Laughlin, G., & Chambers, J. E. 2001, ApJ, 551, L109
Lee, M. H., & Peale, S. J. 2002, ApJ, 567, 596
Lee, M. H., Peale, S. J., Pfahl, E., et al. 2007, Icarus, 190, 103
Leggett, S. K. 1992, ApJS, 82, 351
Leggett, S. K., Allard, F., Geballe, T. R., Hauschildt, P. H., & Schweitzer, A. 2001, ApJ, 548, 908
Li, J., Zhou, L.-Y., & Sun, Y.-S. 2008, Chin. Astron. Astrophys., 32, 409
Libert, A.-S., & Tsiganis, K. 2009, A&A, 493, 677
Marcy, G. W., Butler, R. P., Vogt, S. S., Fischer, D., & Lissauer, J. J. 1998, ApJ, 505, L147
Marcy, G. W., Butler, R. P., Fischer, D., et al. 2001, ApJ, 556, 296
Mardling, R. A. 2007, MNRAS, 382, 1768
Mayor, M., Pepe, F., Queloz, D., et al. 2003, The Messenger, 114, 20
Mayor, M., Bonfils, X., Forveille, T., et al. 2009, A&A, 507, 487
Nagasawa, M., Tanaka, H., & Ida, S. 2000, AJ, 119, 1480
Press, W. H., Teukolsky, S. A., Vetterling, W. T., et al. 1992, Numerical recipes in FORTRAN, 2nd edn. The art of scientific computing (Cambridge: University Press)
Rivera, E. J., & Lissauer, J. J. 2001, ApJ, 558, 392
Rivera, E. J., Lissauer, J. J., Butler, R. P., et al. 2005, ApJ, 634, 625
Thommes, E. W., & Lissauer, J. J. 2003, ApJ, 597, 566
Turon, C., Creze, M., Egret, D., et al. 1993, Bulletin d'Information du Centre de Données Stellaires, 43, 5
Udry, S., Bonfils, X., Delfosse, X., et al. 2007, A&A, 469, L43
Wolszczan, A., & Frail, D. A. 1992, Nature, 355, 145